Mon. Not. R. Astron. Soc. **374,** 823–831 (2007) doi:10.1111/j.1365-2966.2006.11170.x

Is the X-ray spectrum of the narrow emission line QSO PG1211+143 defined by its energetic outflow?

K. A. Pounds[1]★ and J. N. Reeves[2]

[1]*Department of Physics and Astronomy, University of Leicester, Leicester LE1 7RH*
[2]*Laboratory for High Energy Astrophysics, NASA Goddard Space Flight Center, Greenbelt, MD 20771, USA*

Accepted 2006 October 9. Received 2006 September 29; in original form 2006 May 26

ABSTRACT

An *XMM–Newton* observation of the bright QSO PG1211+143 in 2001 revealed a blueshifted absorption line spectrum indicative of a high-velocity radial outflow of highly ionized gas. Unless highly collimated, the outflow mass rate was shown to be comparable to the accretion rate, with mechanical energy a significant fraction of the bolometric luminosity. Analysis of the full *XMM–Newton* data set now allows the wider effects of that energetic outflow to be explored. We find that absorption and re-emission of the primary continuum flux in the ionized outflow, together with a second, less strongly absorbed, continuum component can explain the strong 'soft excess' in PG1211+143 without the extreme velocity 'smearing' in conflict with observed absorption line widths. Previously unpublished data from a second *XMM–Newton* observation of PG1211+143 is shown to be consistent with the new spectral model, finding that the additional continuum component dominates the spectral variability. We speculate that this variable continuum component is powered by the high-velocity outflow.

Key words: galaxies: active – galaxies: individual: PG1211+143 – quasars: general – galaxies: Seyfert – X-rays: galaxies.

1 INTRODUCTION

The luminous QSO PG1211+143 has been observed twice by *XMM–Newton*, in 2001 and 2004. Analysis of the EPIC and RGS spectra from the first observation provided evidence for a highly ionized outflow with a velocity of $\sim 0.09 \pm 0.01c$ (Pounds et al. 2003, hereafter P03), though this high velocity was contested following a careful ion-by-ion modelling of the RGS data (Kaspi & Behar 2006). However, a re-examination of the 2001 EPIC data (Pounds & Page 2006) resolved additional absorption lines in the EPIC MOS spectrum, strengthening the initial claim, and yielding a preferred velocity of $v \sim 0.14c$. Confirmation of the high-velocity outflow is important since, as noted in P03, the mechanical energy in the flow, if not highly collimated, is a significant fraction of the bolometric luminosity of PG1211+143 and could be typical of active galactic nuclei (AGNs) accreting near the Eddington rate (King & Pounds 2003), while also providing an example of the feedback required by the linked growth of supermassive black holes (SMBH) in AGNs with their host galaxy (King 2005).

P03 also found a strong 'soft excess' over a 2–10 keV power-law fit of photon index $\Gamma \sim 1.8$, a typical value for type 1 AGNs, and a broad Fe K emission line. Subsequently, the 2001 EPIC spectrum of PG1211+143 has been used by Gierlinski & Done (2004), and more recently by Schurch & Done (2006), to demonstrate how strong absorption of the intrinsic X-ray continuum in a 'velocity-smeared', high-column, ionized gas could provide an alternative explanation (to Comptonization) for the strong soft excess generally seen in type 1 AGNs (Wilkes & Elvis 1987; Turner & Pounds 1989). A more general study by Chevallier et al. (2006) also considered an ionized reflection origin of the soft excess in AGNs (e.g. Crummy et al. 2006) and concluded that absorption was the more likely cause of a strong soft excess (as in PG1211+143).

In the present paper we use the full *XMM–Newton* data set from both observations of PG1211+143 to re-examine the broad-band X-ray spectrum of PG1211+143, to better understand the structure and dynamics of the outflow, and thereby to assess the conjecture that the massive and energetic outflow substantially defines the emerging spectrum.

We assume a redshift for PG1211+143 of $z = 0.0809$ (Marziani et al. 1996).

2 OBSERVATION AND DATA REDUCTION

PG1211+143 was observed by *XMM–Newton* on 2001 June 15 for ∼53 ks, and again on 2004 June 21 for ∼57 ks. In this paper we mainly use the high signal-to-noise ratio data from the EPIC cameras (Strüder et al. 2001; Turner et al. 2001), but with a crucial constraint on high-resolution spectral features provided by the simultaneous RGS data (den Herder et al. 2001). All X-ray data were first screened

★E-mail: kap@star.le.ac.uk

with the XMM SAS v6.5 software and events selected corresponding to patterns 0–4 (single and double pixel events) for the pn camera and patterns 0–12 for the MOS cameras. We extracted EPIC source counts within a circular region of 45 arcsec radius defined around the centroid position of PG1211+143, with the background being taken from a similar region, offset from but close to the target source. After removal of data during periods of high background the effective exposures for the pn camera were ∼49.5 ks in 2001 and ∼25.2 ks in 2004, with corresponding exposures of ∼103 and ∼81 ks for the combined MOS cameras. Individual spectra were then binned to a minimum of 20 counts per bin, to facilitate use of the χ^2 minimization technique in spectral fitting.

Spectral fitting was based on the XSPEC package (Arnaud 1996), version 11.3. All spectral fits include absorption due to the line-of-sight Galactic column of $N_{\rm H} = 2.85 \times 10^{20}\,{\rm cm}^{-2}$ (Murphy et al. 1996) and errors are quoted at the 90 per cent confidence level ($\Delta\chi^2 = 2.7$ for one interesting parameter).

3 VISUAL EXAMINATION OF THE EPIC DATA

Fig. 1 displays the pn spectra of PG1211+143 from the 2001 and 2004 observations in a way that has become conventional, by first fitting a power law over the 2–10 keV band and then extrapolating this fit to lower energies, revealing the 'soft excess' typical of many type 1 AGNs. This approach, followed by P03 in their initial analysis of the 2001 pn camera data of PG1211+143, yielded a power-law fit over the 2–10 keV band with a 'canonical' photon index of $\Gamma \sim 1.79$, together with an Fe K emission line (apparently with a broad red wing), and a strong soft excess parametrized by a blackbody spectrum of $kT \sim 0.1$ keV. The same approach for the 2004 pn data of PG1211+143 yields a steeper power law ($\Gamma \sim 1.85$) and a less strong 'soft excess' (Fig. 1).

An alternative comparison of the 2001 and 2004 spectra is shown in Fig. 2, which plots the unmodelled, background-subtracted data. Shown in this way, we see the spectral change is actually an increase in flux (from 2001 to 2004) between ∼0.7–2 keV, and a (less obvious) decrease at ∼0.5–0.7 keV. Interestingly, the 2001 and 2004 spectra are essentially identical above ∼3 keV. We choose to show the MOS data in Fig. 2 since, while the broad flux profile is the same, the higher energy resolution of the MOS data shows additional low-energy structure in the 2001 spectrum.

To highlight the broad spectral changes between the 2001 and 2004 data we then directly compared the two data sets, noting, for example, that if absorption is having a controlling effect on the emerging spectrum, it should show up in the way in which individual spectra differ. As variable absorption (multiplicative) spectral components are best seen in the ratio of data sets, we therefore rebinned the EPIC data from 2001 to a minimum of 200 counts per channel, in order to show any broad features more clearly, and then rebinned the 2004 data to have identical energy channels. Dividing the first data set by the second then gave the spectral ratio plot of Fig. 3. The most obvious feature is a broad flux deficit over the ∼0.7–2 keV band, the shape and positioning of which is strongly suggestive of differential absorption by ionized gas, with enhanced absorption in the 2001 spectrum.

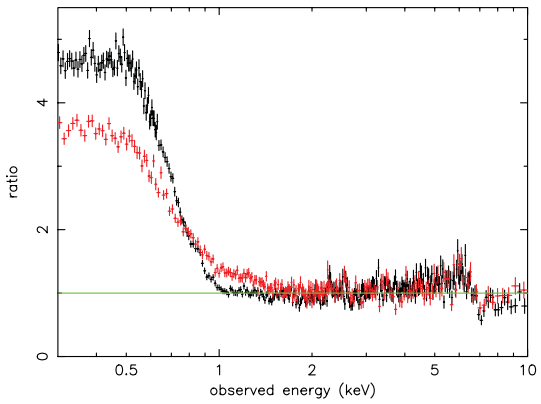

Figure 1. Comparison of the X-ray spectra of PG1211+143 displayed in the conventional way, showing the strong soft excess sitting above a 'canonical' power law, for the pn data from the 2001 (black) and 2004 (red) observations. On this view it appears that the soft excess in 2004 is weaker but 'hotter'.

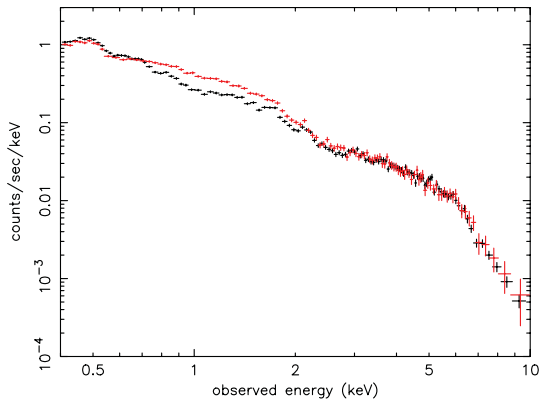

Figure 2. Direct comparison of the background-subtracted MOS data from the 2001 (black) and 2004 (red) observations shows the spectral change to be due to an increase in flux between ∼0.7–2 keV, and a less obvious flux decrease at ∼0.5–0.7 keV.

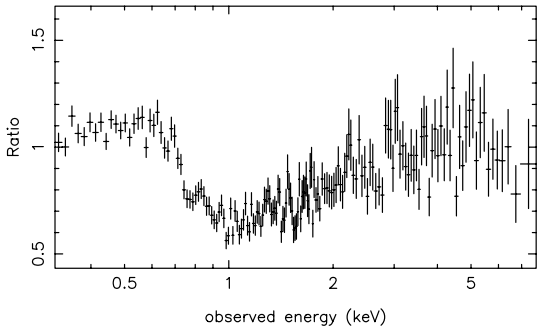

Figure 3. The MOS spectral ratio obtained by dividing the 2001 count rate spectrum by that obtained in 2004. The most obvious feature is a broad deficit at ∼0.7–2 keV indicative of variable photoionized absorption.

Fig. 4 shows the 'difference spectrum', obtained by subtracting the 2004 (background-subtracted) data set from that of 2001. The data have again been rebinned to a minimum of 200 counts per bin. While above ∼2 keV the difference spectrum reflects the very similar hard X-ray fluxes, in addition to a lower flux at ∼0.7–2 keV we see a significant excess peaking at ∼0.5 keV in the 2001 data.

In summary, a direct comparison of the 2001 and 2004 MOS data (comparison of the pn data shows the same features) suggests a decrease in continuum absorption is the main cause of the spectral change in PG1211+143 from 2001 to 2004, together with a decrease in an emission component specific to the soft X-ray band. Implicitly, both results support the contention that reprocessing in ionized gas is a primary factor in determining the form of the observed broad-band X-ray spectrum. An important constraint on the nature of the

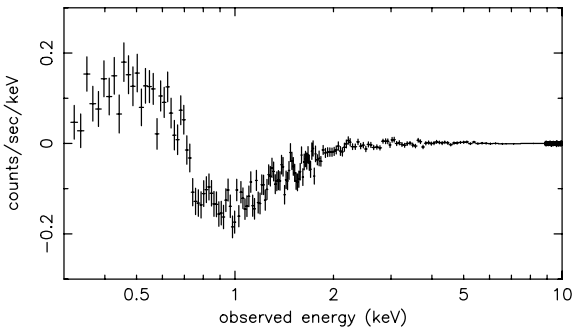

Figure 4. The MOS difference spectrum, obtained by subtracting the 2004 spectrum from that of 2001, shows the near-identical hard X-ray spectra, with a lower flux at ∼0.7–2 keV and comparable higher flux peaking at ∼0.5–0.6 keV in the 2001 observation.

variable absorption is the similarity in the ionizing flux during the 2001 and 2004 observations indicated by the near-identical spectra above ∼3 keV, suggesting a change in covering factor (CF) rather than ionization parameter.

4 THE CASE FOR A FRESH APPROACH TO MODELLING THE X-RAY SPECTRUM OF PG1211+143

Accumulation of high-quality, broad-band X-ray spectra of AGNs, particularly from *XMM–Newton* EPIC, has raised doubts over the physical reality of the soft excess and also the ubiquity of the relativistic Fe K emission line suggested by earlier *ASCA* observations. In particular, the conventional interpretation of the soft excess in type 1 AGNs, as arising by Comptonization of cooler disc photons, has been questioned by Gierlinski & Done (2004).

Those authors studied 26 AGNs from the PG sample observed with XMM, fitting the X-ray spectra with a double Comptonization model. They found that while Comptonization of the accretion disc emission provided a good statistical fit to the soft excess below 2 keV in every case, the temperature of the cool Comptonizing region was remarkably constant over the sample, despite that sample having a large range in mass and luminosity, and hence in disc temperature, and in the ratio of power released in the hot plasma to that from the disc. Given these difficulties, Gierlinski & Done (2004) proposed that the soft excess was an artefact of ionized absorption in a subrelativistic wind above the inner accretion disc. In order to explain the generally smooth form of the soft excess the absorbing gas was required to have a complex velocity structure. Subsequently, Schurch & Done (2006) have explored this 'smeared absorber' model in more detail, showing – in particular – that by including re-emission from the ionized gas the strong soft excess in PG1211+143 could be reproduced.

Chevallier et al. (2006) have also examined alternative origins of the soft excess in AGNs, including enhanced soft X-ray emission from an ionized accretion disc (e.g. Crummy et al. 2006). Chevallier et al. (2006) found that ionized absorption in a high speed outflow, or an inhomogeneous accretion flow could best explain some AGN X-ray spectra, particularly those with very strong soft excesses (as PG1211+143), while only weak excesses can be modelled by reflection unless the primary continuum is strongly depressed (Fabian et al. 2002). However, they concluded that simple 'smeared' absorption models would require 'fine tuning' to constrain the depth of the trough near 1 keV and thereby be generally applicable.

A second spectral feature whose interpretation has been questioned recently is the broad wing seen to the low-energy side of the Fe K fluorescent emission line in a number of bright AGNs. While widely considered to be due to Doppler and strong gravity broadening of radiation reflected off the innermost accretion disc (e.g. Fabian et al. 2000), an alternative explanation as (again) an artefact of absorption has been proposed in specific cases (e.g. Inoue & Matsumoto 2003; Kinkhabwala 2003).

Clarifying the nature of such significant features in the X-ray spectra of AGNs is important to explore the accretion process, outflows of ejected matter, and ultimately the properties of the central black hole. Its strong soft excess, evidence for a massive and energetic outflow, and high accretion ratio make PG1211+143 a particularly interesting object by which to explore an alternative approach to deconvolving the broad-band X-ray spectrum.

5 DEVELOPING A NEW SPECTRAL MODEL FOR THE 2001 OBSERVATION OF PG1211+143

We begin the fresh approach by noting that the intrinsic continuum over the broad X-ray band now visible to *XMM–Newton* might not be adequately described by a simple power law derived by fitting to the data over the ∼2–10 keV band. Recent studies of spectral variability in MCG-6-30-15 (Vaughan & Fabian 2004) and 1H0419-577 (Pounds et al. 2004), among the most detailed broad-band spectral analyses to date, have provided clear evidence of a variable power-law component of slope significantly steeper than the 'canonical value' of $\Gamma \sim 1.9$ (Nandra & Pounds 1994). That finding is important in the present context since, if absorption is to create the impression of a strong 'soft excess', then the underlying continuum must be much steeper than it appears above ∼2 keV. To allow for that possibility, while retaining a harder 'primary' continuum in the range predicted by the disc/corona model (Haardt & Maraschi 1991), we include two power-law components in the new model. For simplicity we will call these the primary and secondary continuum components.

Indication from the flux ratio plot that the main spectral change between the 2001 and 2004 *XMM–Newton* observations of PG1211+143 is due to a change in ionized absorption affecting the spectrum above ∼0.7 keV, suggests the model should include a moderately ionized ('warm') absorber, in addition to the highly ionized absorber responsible for the narrow, blueshifted absorption lines (P03; Pounds & Page 2006). Finally, we include components to model the re-emission from both ionized absorbers.

In XSPEC terms the prospective model is then WA(PO1*ABS1* ABS2 + PO2*ABS3*ABS4 + EM1/3 + EM2/4), where WA represents the line-of-sight Galactic column, included in all fits, and PO1, PO2 are the separate power-law components. ABS1 and 3 represent the high-ionization absorber, differing only in column density on the two continua, while ABS2 and 4 similarly represent the lower ionization absorption. Finally, EM1/3 and EM2/4 model the re-emission from the highly ionized and warm absorbers, respectively. All ABS and EM components are modelled by photoionized gas using the XSTAR code (Kallman et al. 1996). We assume a relatively high turbulent velocity of 1000 km s^{-1} full width at half-maximum (FWHM) in order to allow substantial line opacity before saturation. Free parameters in each XSTAR grid are the column density and ionization parameter, with outflow (or inflow) velocities included as an adjustment to the apparent redshift of the absorbing or emitting gas. All abundant elements from C to Fe are included with the relative abundances as a further variable input parameter, but tied for all the XSTAR components and limited to within a factor

Table 1. Parameters of the model fits to the pn, MOS and RGS data from the 2001 *XMM–Newton* observation of PG1211+143. Power-law indices Γ_1 and Γ_2 refer to the primary and secondary continuum components, respectively. Both high and moderate ionization absorbers affect each continuum component, with equivalent hydrogen column densities in units of 10^{22} cm^{-2} and ionization parameters in erg cm s^{-1}. Effective redshifts and implied velocities from the ionized gas absorption and re-emission spectra are given in the text.

Instrument	Γ_1	$N_{\rm H}$	log ξ	$N_{\rm H}$	log ξ	Γ_1	$N_{\rm H}$	log ξ	$N_{\rm H}$	log ξ	χ^2/d.o.f.
pn	2.2 ± 0.1	5.5	1.43 ± 0.03	3.8	2.9 ± 0.1	3.1 ± 0.1	0.16	1.43 ± 0.03	1.6	2.9 ± 0.1	835/824
MOS	2.2 ± 0.1	2.5	1.53 ± 0.05	6.5	2.8 ± 0.1	3.3 ± 0.1	0.1	1.53 ± 0.05	1.2	2.8 ± 0.1	438/367
RGS	2.2	3.7	1.4 ± 0.1	–	–	3.3 ± 0.2	0.1	1.4 ± 0.1	0.02	2.5 ± 0.1	588/575

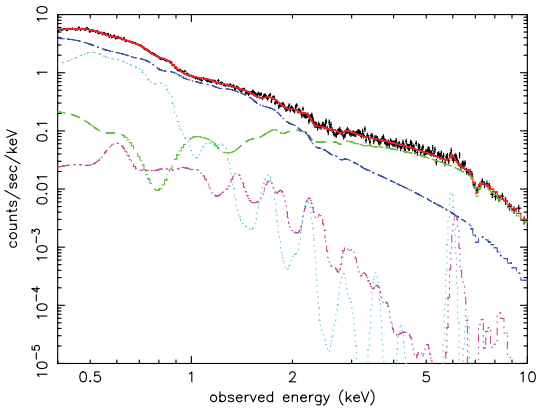

Figure 5. The full spectral model (red) fitted to the 2001 pn camera data of PG1211+143. The model components are the primary power law (green), secondary power law (dark blue), re-emission from the moderately ionized gas (light blue) and re-emission from the highly ionized gas (magenta).

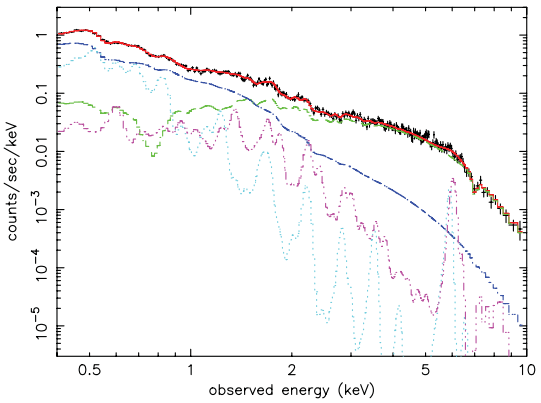

Figure 6. The spectral model (red) fitted to the 2001 MOS camera data of PG1211+143. The model components are primary power law (green), additional power law (dark blue), re-emission from the moderately ionized gas (light blue) and re-emission from the highly ionized gas (magenta).

of 2 of solar. Further constraints on the model are to tie the ionization parameters of ABS1 and 3, and of ABS2 and 4, and also with their respective re-emission spectra.

We first evaluated the model with the pn and MOS data sets, separately, given their differing low-energy responses and the higher MOS resolution, which potentially is important in resolving features in the soft X-ray band (Pounds & Vaughan 2006).

An excellent statistical fit was obtained for the pn data with the component parameters as listed in Table 1. The spectral components are shown together with the total model and pn data in Fig. 5. Fitting the model to the 2001 MOS data yielded similar component parameters, although the statistical quality of the fit was less good. The fit parameters are listed in line 2 of Table 1 and the data, model and separate model components are shown in Fig. 6.

Visual examination of Figs 5 and 6 clarifies the main features of the new model.

Above ∼3 keV the spectrum is dominated by the 'primary' power law, with a photon index $\Gamma \sim 2.2$, at the upper end of – but consistent with – the 'accepted' range for type 1 AGN spectra. At lower energies the secondary power-law component ($\Gamma \sim 3.1$) is more important, while below ∼1 keV re-emission, particularly from the 'warm' absorber, becomes significant. We note that variability in this component between 2001 and 2004 could explain the low-energy peak in the difference spectrum of Fig. 4.

Strong absorption of the primary power law is seen to be responsible for the mid-band (∼2–6 keV) spectral curvature, with ionized gas column densities of $N_{\rm H} \sim 3$–5×10^{22} cm^{-2}. In both pn and MOS spectral fits the model shows a broad trough near ∼0.8 keV, due to Fe L absorption. Fig. 3 shows a similar spectral feature in the 2001/2004 ratio plot, again indicating lower absorption in the second observation.

The secondary power-law continuum appears to suffer much less absorption, with a negligible warm absorber column and a factor of ∼2–5 lower column density of highly ionized absorber.

The high-velocity, high-ionization absorber produces the narrow absorption lines reported in PO3 (with revised identifications in Pounds & Page 2006), while dilution by the steep power-law component could explain the weakness of narrow absorption lines in the RGS data (P03; Kaspi & Behar 2006).

5.1 Velocity structure

The velocity structure of the photoionized gas components is of particularly interest and relies on identifying significant spectral structure in the data. Our approach in P03 and in Pounds & Page (2006) was based on the visual identification of narrow absorption lines, backed up by modelling with XSTAR. While that works well where the aim, as there, was to determine the velocity of a strong outflow, here we have to rely principally on modelling to interpret the multicomponent broad-band spectrum of PG1211+143. For the highly ionized absorber, the high velocity is again constrained by the presence of narrow absorption lines in the EPIC data, with the highly ionized XSTAR component having an apparent blueshift (in the observer frame) of $\sim 0.06 \pm 0.01$, indicating an outflow velocity (in the AGN rest frame) of $v \sim (0.14 \pm 0.01)c$. For the warm absorber the XSTAR fits yield apparent redshifts of $\sim 0 \pm 0.02$ (pn) and $\sim 0.02 \pm 0.02$ (MOS). Constraints on the velocity of this moderately ionized absorber are less secure, being derived from fitting the mid-band spectral curvature and the rather complex absorption

structure below ∼2 keV where the ionized gas recovers transparency. The column density and ionization parameter also affect the spectral curvature while, at lower energies, the re-emission spectrum has overlapping spectral structure. It does appear, however, that the moderately ionized gas is outflowing at a somewhat lower, but still high velocity.

In contrast, the emission line spectra in both pn and MOS models prefer a low mean velocity in the rest frame of the galaxy, with an apparent redshift of the XSTAR emission spectra of ∼0.07 ± 0.01, corresponding to a mean outflow velocity in the rest frame of PG1211+143 of ∼3000 ± 3000 km s^{-1}. Visual examination of the spectral components in Figs 5 and 6 suggests the velocity sensitivity of the emission line gas derives from the strong O VII and O VIII lines at ∼0.5 and ∼0.6 keV.

5.2 Component luminosities, absorption and re-emission

Overall and component luminosities in the pn and MOS model fits are sufficiently similar to take their average values. For the 2001 observation we find an overall luminosity $L_{0.4-10} \sim 1.2 \times 10^{44}$ erg s^{-1}, with a 2–10 keV luminosity $L_{2-10} \sim 5.0 \times 10^{43}$ erg s^{-1}. The primary power law is the dominant component with $L_{0.4-10} \sim 5 \times 10^{43}$ erg s^{-1}; this increases to ∼1.3 × 10^{44} erg s^{-1} when corrected for absorption (90 per cent being in the moderately ionized absorber). The secondary power law has an observed luminosity $L_{0.4-10} \sim 6 \times 10^{43}$ erg s^{-1}, increasing to ∼7 × 10^{43} erg s^{-1} when corrected for absorption.

Re-emission from the ionized outflow provides a strong contribution to the observed soft X-ray flux below ∼1 keV, with an integrated luminosity in the emission line spectrum $L_{\rm em} \sim 1.8 \times 10^{43}$ erg s^{-1} in the moderately ionized component and $L_{\rm em} \sim 1.5 \times 10^{42}$ erg s^{-1} in the high-ionization component. Comparing the absorbed and re-emitted luminosities we estimate the covering fractions (CFs), for an optically thin radial flow, of ∼0.2 and ∼0.1 for the warm and highly ionized gas components, respectively.

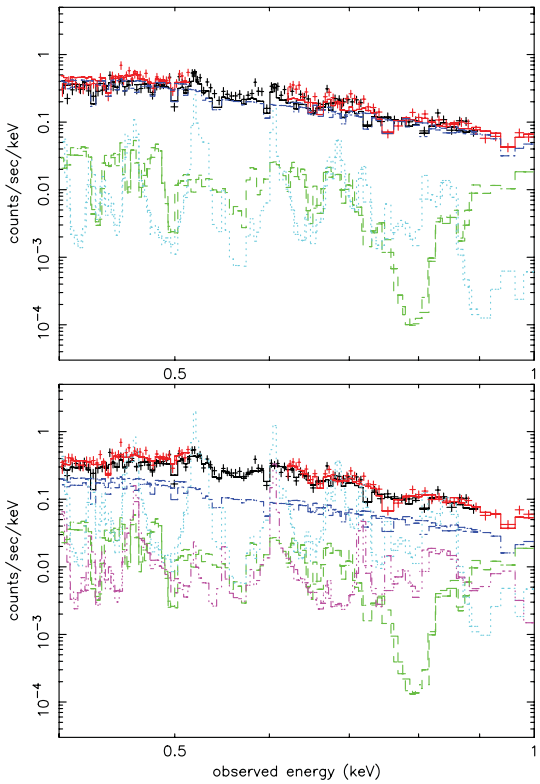

Figure 7. The spectral model fitted to the 2001 RGS data of PG1211+143. The upper panel shows the fit with no added line broadening; the lower panel includes a Gaussian smoothing of the emission line spectrum providing a much better fit as described in Section 6. The RGS data and overall model fits are shown in red and black, while the separate model components are the absorbed primary power law (green), secondary power law (dark blue) and input emission line spectra for the warm (light blue) and highly ionized (magenta) gas.

6 CHECKING FOR CONSISTENCY WITH THE RGS SPECTRUM OF 2001

A key constraint of the new spectral model is to produce a strong soft excess with no strong narrow spectral lines in absorption or emission, although there should be weak absorption lines imposed in the soft band by the highly ionized, high-velocity flow. Several such lines, at low signal-to-noise ratio in the RGS data, were claimed in our initial analysis reported in P03.

Examination of Figs 5 and 6 suggest the narrow absorption line spectrum would be significantly 'diluted' by the dominance, at low energies, of the weakly absorbed secondary power-law continuum. However, the absence of strong, narrow emission lines in the RGS spectrum requires substantial line broadening of the re-emission component in the EPIC model spectrum. Conceivably this could be a result of a high-velocity flow integrated over a wide angle, which would be consistent with the estimated CF of ∼0.2, for a partially filled outflow.

The high intrinsic resolution of the RGS therefore offers a valuable check on the model spectrum of PG1211+143 over the soft X-ray band, even if the emission lines are strongly broadened. Testing the model against the RGS data from the 2001 observation initially gave an unacceptable [χ^2 per degree of freedom (d.o.f.) = 845/636], with the steep power law ($\Gamma \sim 3$) dominant. Examination of the data:model residuals showed this to be due to substantial low-energy structure, too broad to be fitted by the narrow line input spectrum of the XSTAR model. We therefore added a Gaussian smoothing factor to the emission line component in the model (gsmooth in XSPEC). The broadened emission lines now increased in strength to match the observed spectral structure, with the power-law component becoming correspondingly weaker, yielding an excellent fit (χ^2 per d.o.f. = 649/635 over the 0.35–1.5 keV band). Both unsmoothed and smoothed spectral fits are reproduced in Fig. 7, where the soft X-ray emission can be identified in the figure, in order of increasing energy, with K-shell emission of N, O and Ne, together with several strong Fe L lines. The apparent redshift from the XSTAR emission spectrum fit of ∼0.08 ± 0.01 was consistent with the EPIC data fits, while – encouragingly – the RGS data also requires a steep power-law component ($\Gamma \sim 3.3 \pm 0.2$).

Fig. 8 provides another view of the spectral structure in the soft X-ray band, showing the broad spectral lines that are successfully modelled by re-emission from the ionized gas in PG1211+143. The best-fitting Gaussian ($\sigma \sim 25$ eV at 0.6 keV), would correspond to velocity broadening of 29 000 km s^{-1} FWHM, which again would suggest the high-velocity flow occurs over a wide angle. Much better data will be required to determine the true emission line profiles and constrain the effects of saturation in the principal resonance lines.

The important point for the present study is that the spectral model developed to fit the EPIC data is fully consistent with the RGS data provided the emission lines are strong but broad. In addition, the RGS spectral fit requires a steep power-law continuum,

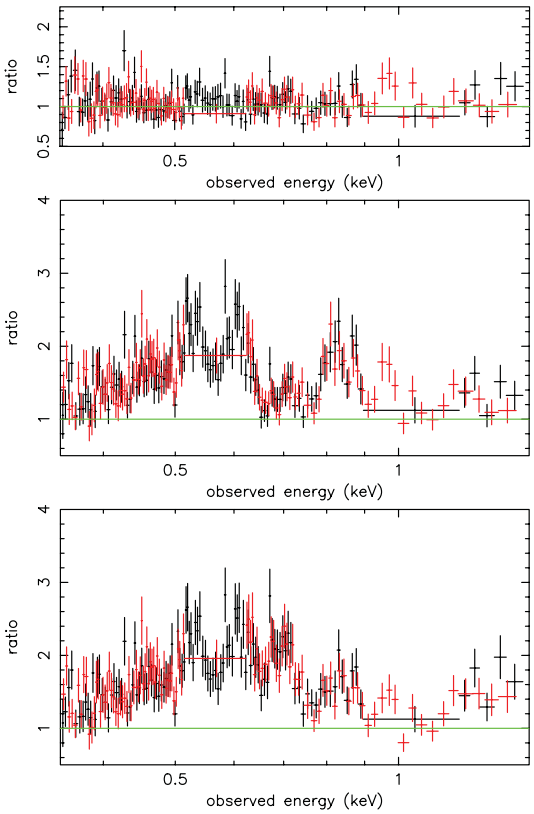

Figure 8. (Upper panel) Ratio of the RGS data to the model described in Section 6. The mid-panel shows the data:model ratio when the metals C–Mg are removed from the XSTAR emission line spectra, revealing four broad peaks corresponding (from the left) to resonance line emission from N VII, O VII, O VIII and Ne IX. The lower panel shows the same data:model ratio when Fe is also removed from the emission line spectra, yielding a further broad excess at ∼0.7 keV due to Fe L emission.

making a significant contribution to the observed soft X-ray flux below ∼1 keV. The integrated luminosity in the RGS emission line spectrum, of $L_{\rm em} \sim 1.8 \times 10^{43}$ erg s^{-1}, is consistent with the values derived from the EPIC spectral fits. To place the soft X-ray emission in a wider context we note it represents some 0.5 per cent of the bolometric luminosity of PG1211+143. In comparison, an *XMM–Newton* observation of NGC1068, a Seyfert 2 galaxy with a similar bolometric luminosity, found an integrated soft X-ray emission luminosity of only $\sim 5 \times 10^{41}$ erg s^{-1} (Pounds & Vaughan 2006). The much stronger soft X-ray line emission from PG1211+143 supports the view of a strong centrally condensed emission region that would be hidden from view in a Seyfert 2.

7 APPLYING THE NEW SPECTRAL MODEL TO THE 2004 OBSERVATION OF PG1211+143

As the new spectral model was based on the evidence for variable ionized absorption, and re-emission, from a direct comparison of the 2001 and 2004 data sets it is clearly important to show that the 2001 model parameters can be varied in a physically reasonable way to also describe the 2004 spectra.

To that end we tested the new spectral model with the 2004 data of PG1211+143, keeping the element abundances in XSTAR and ionization parameters unchanged. Justification for the constant ionization parameters is based on the near-identical hard X-ray fluxes

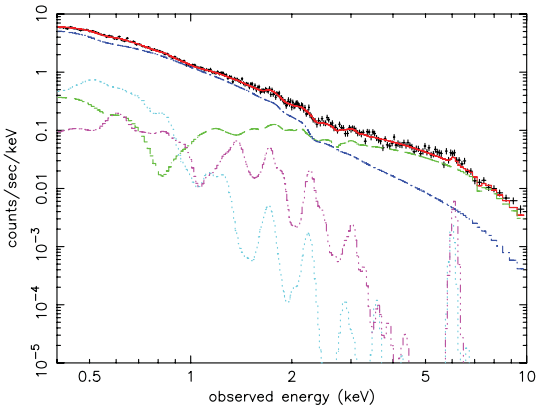

Figure 9. The spectral model fitted to the 2004 pn camera data of PG1211+143. The model components are primary power law (green), additional power law (dark blue), re-emission from the moderately ionized gas (light blue) and re-emission from the highly ionized gas (magenta).

(which we take as a good proxy for the ionizing luminosity). Fig. 9 illustrates the fit and the separate model components for the 2004 pn data, which yielded an acceptable χ^2 per d.o.f. = 691/625. The fit to the 2004 MOS data was statistically excellent, with χ^2 per d.o.f. = 350/351, as was that to the 2004 RGS data. Comparing the 2001 and 2004 model fits to both EPIC and RGS data shows that the spectral change is primarily due to a stronger secondary power-law component, though the 'warm' absorption of the primary power law and the soft X-ray line emission also appear to be weaker. The column density of the highly ionized absorber is a factor of ∼2 lower, consistent with the significantly weaker absorption line at ∼7 keV in 2004. Dilution by a stronger steep power-law continuum and weaker line emission both contribute to the reduced soft X-ray structure evident in the 2004 RGS spectrum (Fig. 10).

In summary, we find reasonable changes in the 2001 spectral model also fit the 2004 data. The net effect of a stronger secondary power law, with reduced ionized absorption (and re-emission) can satisfactorily match the ratio and difference spectra shown in Figs 3 and 4. However, given the relative complexity of the spectral deconvolution we stress that more than two spectral 'snapshots' will be required to fully resolve and understand the spectral variability. For example, while our modelling suggests the reduced soft X-ray structure in the 2004 spectrum is a combination of a stronger continuum and weaker line emission, we would expect further observations to show this to be coincidental.

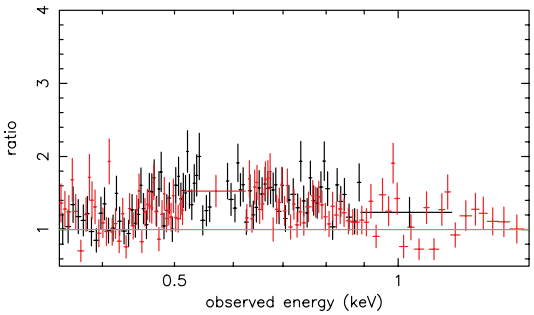

Figure 10. Ratio of the 2004 RGS data to the model shown in Fig. 9 when the metals C–Fe are removed from the XSTAR emission line spectra. Although spectral structure is seen, it is at a significantly lower level than in the corresponding plot for the 2001 RGS data (Fig. 8, lower panel).

8 DISCUSSION

We have explored a new model to describe the complex broad-band X-ray spectrum of the narrow emission line QSO PG1211+143. The model structure was guided by a comparison of the spectral data from two *XMM–Newton* observations of PG1211+143 in 2001 and 2004, which suggested a reduction in ionized absorption (and re-emission) in the latter case. In addition, the model allows for a second continuum component, described by a steeper power law, to take account of evidence from other AGN studies that a steep power law can be a principal contributor to spectral variability. Although more complex than the conventional description of the X-ray spectrum of PG1211+143, where the hard power law and strong 'soft excess' are both modelled by Comptonization of soft accretion disc photons, the new model is encouragingly self-consistent. Thus, the main continuum absorption is modelled by moderate ionization (warm) matter of column density $N_{\rm H} \sim 3 \times 10^{22}$ cm^{-2} and log $\xi \sim 1.4$, with re-emission from gas of the same ionization parameter dominating the observed spectral structure below $\sim$1 keV. Modelling the higher resolution RGS data confirms the contributions of the broadened emission lines and the steep power-law continuum to the soft X-ray spectrum of PG1211+143. From a comparison of the absorbed and re-emitted luminosities we find CFs of $\sim$0.2 and $\sim$0.1, respectively, for the warm and highly ionized outflows. In turn, the mechanical energy in the highly ionized outflow is confirmed to be an order of magnitude larger than the luminosity in the secondary power law, supporting our conjecture that shocks in the outflow could drive that additional continuum component.

Application of the 2001 spectral model to the 2004 data suggests the primary change is due to an increase in the steep power-law continuum rather than a decrease in absorption of the primary power law. In fact, given the quality of the shorter 2004 observation, it is possible the ionized absorption did not change, a possibility consistent with the very similar ionizing fluxes indicated by the comparable hard X-ray spectra which would have required a change to be mainly in column density (or CF). A more extended observation of PG1211+143, exploring spectral variability over hours to days, would be very interesting.

8.1 The ionized outflow

The spectral curvature near $\sim$1 keV, previously seen as the onset of a strong 'soft excess' in PG1211+143, is attributed in our model primarily to absorption and re-emission in a substantial column density ($N_{\rm H} \sim$ few times 10^{22} cm^{-2}) of moderately ionized gas. Although not as well constrained as the high-ionization gas, which produces an array of narrow absorption lines (Pounds & Vaughan 2006), the warm absorber also appears to be outflowing at a high velocity. With the present 'snapshot' spectra it is not clear how these absorption components might be related; perhaps they simply represent different matter densities in a common flow.

Identifying the strong absorption line observed at $\sim$7 keV with Fe XXV Heα (here and in Pounds & Page 2006) increases the velocity of the highly ionized outflow from $\sim(0.09 \pm 0.01)c$ (P03) to $v \sim (0.14 \pm 0.01)c$, with a corresponding reduction in the ionization parameter (and column density) from the XSTAR modelling. These changes can then be applied to the radiatively driven wind model discussed in P03 and King & Pounds (2003).

With an ionizing X-ray luminosity ($\geqslant$7 keV) of 3×10^{43} erg s^{-1} and ionization parameter $\xi (= L/nr^2) \sim 1000$, we have $nr^2 \sim 3 \times 10^{40}$ cm^{-1}. Assuming a spherically symmetric flow, at an outflow velocity of $0.14c$, the mass-loss rate is then of the order of $\dot{M} \sim 35b$ M$_\odot$ yr^{-1}, where $b \leqslant 1$ allows for the collimation of the flow. From a comparison of absorbed and re-emitted luminosities in the present analysis we found $b \sim 0.1$, yielding an outflow mass rate $\dot{M} \sim 3.5$ M$_\odot$ yr^{-1}. This compares with $\dot{M}_{\rm Edd} = 1.6$ M$_\odot$ yr^{-1} for a non-rotating SMBH of mass $\sim 4 \times 10^7$ M$_\odot$ (Kaspi et al. 2000) accreting at an efficiency of 10 per cent.

The mechanical energy is now $\sim 10^{45}$ erg s^{-1}, a factor of $\sim$15 larger than the luminosity in the steep power-law component. The ratio of mechanical energy to the bolometric luminosity remains (as in P03) roughly consistent with the value v/c predicted for a radiatively driven outflow (King & Pounds 2003). Again, if the higher velocity equates to the escape velocity at the launch radius $R_{\rm launch}$ (from an optically thick photosphere or radiatively extended inner disc), $v \sim 0.14c$ corresponds to $R_{\rm launch} \sim 50R_{\rm s}$ (where $R_{\rm s} = 2GM/c^2$ is the Schwarzschild radius), or 3×10^{14} cm. The EPIC data show significant flux variability in the harder (2–10 keV) band on time-scales of 2–3 h (Fig. 1 in P03), which would be compatible with the above scale size relating to the primary (disc/corona) X-ray emission region.

Below $\sim$1 keV we find a similar time-scale of variability, but with reduced amplitude. The simplest interpretation is that the photoionized emission is constant over hours, implying that the secondary power-law component is also produced close to the inner disc. Better data will be needed to clarify the time variability and scale size of the separate model components.

We have very little information on the geometry of the warm outflow, responsible for most of the continuum absorption (and re-emission), except that it presumably originates close to the black hole (from its apparent high velocity) and is largely confined within a radius of $\sim$1 pc (by comparison with the much weaker soft X-ray emission seen from Seyfert 2 galaxies). The observed soft X-ray luminosity of $L_{\rm em} \sim 2 \times 10^{43}$ erg s^{-1} corresponds to an emission measure $\Sigma n^2\, V \sim 10^{66}$ cm^{-3} for a solar abundance gas with ionization parameter $\xi \sim 25$. With an ionizing luminosity $\sim 10^{44}$ erg s^{-1}, the ionization parameter gives $nr^2 \sim 4 \times 10^{42}$. Assuming a spherical shell of radius r, thickness δr and density n, a second constraint is the measured column density $n\delta r \sim 4 \times 10^{22}$ cm^{-2}. Interestingly, these parameters match the above emission measure independent of the assumed scale size. For example, assuming $r \sim 10^{16}$ cm, we find $n \sim 4 \times 10^{10}$ cm^{-3} and $\delta r \sim 10^{12}$ cm. For $r \sim 10^{17}$ cm, an alternative set of self-consistent parameters are $n \sim 4 \times 10^8$ cm^{-3} and $\delta r \sim 10^{14}$ cm.

Although the above estimates are very crude, we note the relatively high densities are essential for much of the gas to remain in a state of moderate ionization so close to the powerful continuum source. A likely geometry may be for the warm gas to exist in many, dispersed small clouds rather than the thin spherical shell assumed above.

That would extend the picture developed in P03 and King & Pounds (2003) to incorporate higher density 'clouds' entrapped in the fast outflow and responsible for the strong low-energy absorption (and re-emission) previously interpreted as the 'soft excess'. A possible scenario might be where an inhomogeneous flow accretes through the inner disc to a radius R where radiation pressure causes the matter to be launched at the local escape velocity. As the outflow expands outwards the mean density will fall, as will the filling factor of the cooler, more opaque, matter. If the secondary power law is indeed formed by shocks in the fast outflow, then a centrally condensed absorber could explain the stronger absorption

we find on the primary power-law continuum (assumed to form in the disc/corona).

8.2 The second power-law component

The incentive for including a second power-law component derived mainly from the detailed studies of MCG-6-30-15 (Vaughan & Fabian 2004) and 1H 0419-577 (Pounds et al. 2004), where difference spectrum analyses showed the primary spectral change in each case could be attributed to a variable flux, steep power law. It is also interesting to recall that a 'broken power law', with a steeper component at lower energies has often been used to parametrize AGN spectra, without any physical explanation being offered. In the present study of PG1211+143 we find the inclusion of a second continuum component provides the simplest variable to allow a good fit to both 2001 and 2004 EPIC data. In contrast, a reduction in the CF (modelled by a lower column) of ionized absorber on the primary power law is not able – alone – to fit both data sets.

A further reason to include the second power-law component in our modelling was to quantify the conjecture that the mechanical energy in the high-velocity outflow in PG1211+143 might power a continuum component additional to primary disc/coronal emission. A key factor in determining the mass and energy in the outflow is the degree of collimation. Our modelling of the broad-band spectrum of PG1211+143 has quantified both the absorbed and re-emitted fluxes for the ionized outflow and thereby allowed the CFs (or fractional solid angle) of to be estimated. With a CF of $\sim$0.1, we have seen that the mechanical energy in the fast, highly ionized outflow is ample to power the second continuum (steep power-law) component. Few hours variability below $\sim$1 keV, although of lower amplitude than in the harder X-ray band, suggests the second continuum component originates at a small radius. If powered by the fast outflow, possibilities might be internal shocks in the flow (perhaps analogous to the process suggested in gamma ray bursts), or by running into the slower moving clouds providing the bulk of the continuum opacity. A possible X-ray emission mechanism in either case could be Comptonization of optical–UV disc photons, where the steep power law would be a result of the relatively lower energy content of the electron 'corona' compared with that responsible for the primary power-law continuum.

9 A REVISED ASSESSMENT OF AGN X-RAY SPECTRA

In contemplating how widely applicable our new model might be to describing the X-ray spectra of type 1 AGNs, we note that a bolometric luminosity of the order of 4×10^{45} erg s^{-1} and reverberation mass estimate for the SMBH in PG1211+143 of $M \sim 4 \times 10^7$ M$_\odot$ (Kaspi et al. 2000) indicates PG1211+143 is accreting close to the Eddington rate. Additional support for that view comes from the optical classification of PG1211+143 as a Narrow Line Seyfert, now thought to be a characteristic of a high accretion ratio (e.g. Pounds & Vaughan 2000 and references therein). King & Pounds (2003) provided a simple physical model whereby massive, high-velocity outflows can be expected in AGNs accreting at or above the Eddington limit. PG1211+143 may therefore be a special case among bright, nearby AGNs.

However, it is intriguing that the X-ray spectra of many bright type 1 AGNs have a similar profile to that of PG1211+143 shown in Fig. 1, suggesting ionized absorption is a common cause of the 'soft excess'. An alternative model that works well for weaker soft excesses invokes strong photoionized reflection (Crummy et al. 2006), where the smooth spectral profile is explained by relativistic broadening in the inner disc.

Further observations of PG1211+143, extended over several days, are essential to test the new spectral model, in particular to resolve the contributions of variable absorption (and re-emission) from ionized gas to the overall spectral form. The variability timescale of the secondary power law will constrain the scale of the region where we predict the fast outflow undergoes internal shocks. Detecting hard X-ray emission from PG1211+143 above $\sim$20 keV would also support the need for a continuum component with photon index less steep than that in the single power-law/absorption models (Gierlinski & Done 2004; Schurch & Done 2006). Finally, much deeper RGS spectra are needed to resolve the broad emission line profiles indicated in the model fits.

10 SUMMARY

(1) Previous analyses of the 2001 *XMM–Newton* observation of the bright quasar PG1211+143 have reported evidence of a high-velocity ionized outflow (P03; Pounds & Page 2006). By deconvolving the absorption and emission luminosities in the broad-band spectrum, we now find a CF of the order of $\sim$0.1 for the fast outflow, confirming the mass rate and mechanical energy to be comparable to the accretion rate and bolometric luminosity, respectively.

(2) We show that an additional outflow component of less highly ionized (and hence more opaque) gas can impose significant curvature on the emerging spectrum near $\sim$1 keV, thereby replicating a 'soft excess' when applied to a continuum steeper than the canonical value.

(3) Narrow absorption lines in the EPIC spectra show the outflow to be approximately radial, in contrast with the assumption of a relativistically smeared absorber in the soft excess modelling of Schurch & Done (2006).

(4) However, like Schurch & Done (2006), we find that re-emission of the absorbed continuum also makes a significant contribution to the observed soft X-ray flux. The high integrated luminosity of the photionized outflow in PG1211+143 is more than an order of magnitude larger than that of NGC 1068, a Seyfert 2 galaxy of comparable bolometric luminosity, consistent with an expanding flow originating close to the SMBH.

(5) Inclusion of a secondary continuum component, which energetically could be powered by the high-velocity outflow, is supported by a fit to the soft X-ray spectrum of the RGS. The RGS analysis also requires the soft X-ray line emission to be strongly broadened, possibly by a combination of velocity broadening and line saturation.

(6) Testing the resulting model with data from a second *XMM–Newton* observation of PG1211+143 in 2004 shows that the spectral change is dominated by an increase in the secondary power-law component, which mimics the effect of reduced ionized absorption of the primary continuum.

(7) A further interesting consequence of the double power-law model is to remove the conceptual difficulty in considering partial covering as an alternative to the extreme relativistic Fe K emission line apparent in a simple power-law fit (P03).

(8) We suggest that the above model could be generally applicable to type 1 AGNs accreting at or above to the Eddington limit.

ACKNOWLEDGMENTS

The results reported here are based on observations obtained with *XMM–Newton*, an ESA science mission with instruments and

contributions directly funded by ESA Member States and the USA (NASA). The authors wish to thank the SOC and SSC teams for organizing the *XMM–Newton* observations and initial data reduction.

REFERENCES

Arnaud K. A., 1996, in Jacoby G. H., Barnes J., eds, ASP Conf. Ser. Vol. 101, Astronomical Data Analysis Software and Systems. Astron. Soc. Pac., San Francisco, p. 17
Chevallier L., Collin S., Dumont A. M., Czerny B., Mouchet M., Goncalves A. C., Goosmann R., 2006, A&A, 449, 493
Crummy J., Fabian A. C., Brandt W. N., Boller Th., 2006, MNRAS, 361, 1197
den Herder J. W. et al., 2001, A&A, 365, L7
Fabian A. C., Iwasawa K., Reynolds C. S., Young A. J., 2000, PASP, 112, 1145
Fabian A. C., Ballantyne D. R., Merloni A., Vaughan S., Iwasawa K., Boller Th., 2002, MNRAS, 331, L35
Gierlinski M., Done C., 2004, MNRAS, 349, L7
Haardt F., Maraschi L., 1991, ApJ, 350, L81
Inoue H., Matsumoto C., 2003, PASJ, 55, 625
Kallman T., Liedahl D., Osterheld A., Goldstein W., Kahn S., 1996, ApJ, 465, 994
Kaspi S., Behar E., 2006, ApJ, 636, 674
Kaspi S., Smith P. S., Netzer H., Maoz D., Jannuzi B. T., Giveon U. et al., 2000, ApJ, 533, 631
King A. R., 2005, ApJ, 635, L121
King A. R., Pounds K. A., 2003, MNRAS, 345, 657
Marziani P., Sulentic J. W., Dultzin-Hacyan D., Clavani M., Moles M., 1996, ApJS, 104, 37
Mason K. O. et al., 2001, A&A, 365, L36
Murphy E. M., Lockman F. J., Laor A., Elvis M., 1996, ApJS, 105, 369
Nandra K., Pounds K. A., 1994, MNRAS, 268, 405
Pounds K. A., Page K. L., 2006, MNRAS, 372, 1275
Pounds K. A., Vaughan S., 2000, New Astron. Rev., 44, 431
Pounds K. A., Vaughan S., 2006, MNRAS, 368, 707
Pounds K. A., Reeves J. N., King A. R., Page K. L., O'Brien P. T., Turner M. J. L., 2003, MNRAS, 345, 705 (P03)
Pounds K. A., Reeves J. N., Page K. L., O'O'Brien P. T., 2004, ApJ, 616, 696
Schurch N. J., Done C., 2006, MNRAS, 371, 81
Strüder L. et al., 2001, A&A, 365, L18
Turner T. J., Pounds K. A., 1989, MNRAS, 240, 833
Turner M. J. L. et al., 2001, A&A, 365, L27
Vaughan S., Fabian A. C., 2004, MNRAS, 348, 1415
Wilkes B. J., Elvis M., 1987, ApJ, 323, 343

This paper has been typeset from a TEX/LATEX file prepared by the author.